

Hysteretic Conformational Transition of Single Flexible Polyelectrolyte under Resonant AC Electric Polarization

Shengqin Wang, Hsueh-Chia Chang, and Yingxi Zhu*

Department of Chemical and Biomolecular Engineering,
University of Notre Dame, Notre Dame, Indiana 46556

Received July 13, 2010

Revised Manuscript Received August 13, 2010

There is growing interest in modifying the conformational structures of polyelectrolytes, whose repeating monomers bear ionizable groups in aqueous media. Effective and reversible structural manipulation of polyelectrolytes, including proteins and DNAs, is important not only to fundamentally understand many biomacromolecular processes, such as protein folding and DNA packaging into chromosomes, but also to broad applications from emerging bionanotechnology to energy conversion.^{1–4} As these conformations are realizable in nature, their free energies and the energy barriers between them are often of the order of thermal energy, $k_B T$. Because the adopted conformations of polyelectrolytes are highly sensitive to the local electrostatic environment, dc or low-frequency ac electric fields have been used to manipulate polyelectrolyte chains in aqueous solutions by redistributing counterions surrounding the polyelectrolyte backbones.⁵ However, the large forces of dc mean fields, with corresponding energies larger than thermal noise, often remove the possibility of multiple free energy minima with different molecular conformations, thus preventing reversible and hysteretic transitions between different molecular conformation states—although hydrodynamic or field screening effects can produce hysteretic changes in the molecular dimension or hydrodynamic radius.^{6,7} Moreover, dc or low-frequency ac electric fields produce net electro-osmotic flow and electrode redox reactions, which can camouflage the direct effect of the electric field on the polyelectrolyte conformation.⁸ In this work, we employ spatially uniform ac fields of high frequency to induce the conformational changes in single flexible polyelectrolyte chains, such that ac-electrokinetic-induced flow and Faradaic reactions are eliminated to preserve thermal noise-driven conformational transitions.

Recent polarization experiments with ac frequencies beyond the inverse charge relaxation time of the molecules, that is, the RC (resistance–capacitance) time required for the molecules to neutralize any field-induced charge polarization, suggest that high-frequency ac field is more effective in depleting or concentrating the counterions around nanocolloids and molecules with capacitive charging ion currents.^{9,10} As such dynamic polarization is transient, the hysteretic molecular conformation transitions should be retained but converted to that with respect to frequency variation. We augment this strong high-frequency ac polarization of counterions to induce charge density changes along the polyelectrolyte. The charge polarization of polyelectrolytes under dc or low-frequency ac fields has been theoretically studied and reviewed.^{11–13} Yet prior work has mainly focused on “strong” polyelectrolytes whose charges are fixed and neutralized by the localized counterions, known as “condensed counterions”. The effect of ac electric fields is thus limited to mobile counterions

in the diffusive double layer and not the condensed ones in the Stern layer, resulting in simply modifying the screening ion cloud near a polyelectrolyte without fundamentally changing its charge density. However, for the large class of “weak” polyelectrolytes, whose charges are mobile and highly tunable by the local counterion concentration, their polarization and resulting conformational dynamics under an ac field could be drastically different and yet remains poorly understood. Field-induced counterion dissociation and condensation are expected to sensitively produce nonuniform charge density variation (to the extent of inverting the charge) along the backbones of such polyelectrolytes and can hence readily induce reversible thermal noise-driven polyelectrolyte conformational transitions—not just changes in the radius of gyration.

The coil-to-globule transition (CGT) of polyelectrolytes is considered to be a complicated process governed by charge fraction, molecular architecture, and intermolecular interactions.¹⁴ In contrast to a gradual CGT process for flexible neutral polymers, an abrupt first-order CGT has been predicted by theory and computer simulation^{15–17} but is only confirmed until recently in single-molecule experiments by using AFM¹⁸ and fluorescence correlation spectroscopy (FCS).¹⁹ The CGT of polyelectrolytes can be realized by varying the pH or ionic strength or adding condensing agents,^{19–21} which inevitably modify the solution chemistry to make the transition highly irreversible. In this Communication, we report a reversible and gradual ac-field-induced CGT of a synthetic weak polyelectrolyte, poly(2-vinylpyridine) (P2VP), in dilute aqueous solutions at varied ac frequency, ω , and strength, E_{pp} , by using FCS at a single molecule resolution (see Supporting Information for experimental details).

Briefly, the experimental setup of one-photon FCS is based on an inverted microscope (Zeiss Axio A1) equipped with an oil-immersion objective lens (100×, NA = 1.4). The tiny fluctuations, $I(t)$, in fluorescence intensity, due to the motion of fluorescent molecules in and out of the laser excitation volume, with an Ar laser (Melles Griot, $\lambda = 488$ nm) are measured by two single-photon counting modules (Hamamatsu) independently in a confocal detection geometry at a sampling frequency of 100 kHz in this work. The autocorrelation function, $G(\tau)$, of measured $I(t)$ as^{22–24}

$$G(\tau) = \langle \delta I(t)\delta I(t+\tau) \rangle / \langle I(t) \rangle^2 \quad (1)$$

where $\delta I(t) = I(t) - \langle I(t) \rangle$, is thus obtained by using a multi-channel FCS data acquisition board and its software (ISS)^{19,22} via cross-correlation analysis, which removes the artifacts from detectors, to extract the diffusion coefficient, D , and concentration, $[c]$, of fluorescent molecules under varied experimental conditions. The excitation focal volume is calibrated at the room temperature (~ 25 °C) by Rhodamine 6G of known D ($= 280 \mu\text{m}^2/\text{s}$) in a dilute aqueous solution to be $\bar{w} \approx 260$ nm in the lateral dimension and $z \approx 2 \mu\text{m}$ in the vertical dimension.

We start with P2VP of $M_n = 135\,000$ g/mol in aqueous solutions of constant pH = 4.16, close to its transition pH, pH_{CGT} = 4.20 (see Supporting Information Figure 1), giving initial P2VP coils of a measured hydrodynamic radius, $R_H = 22.5$ nm. The amino end group of P2VP chains is labeled with a bright and stable fluorescence dye, Alexa Fluor 488 (Invitrogen), for the FCS experiments, and excess free dyes are thoroughly removed by size exclusion chromatographic column and further verified by FCS. The lower and upper ω are set between 5 kHz and 10 MHz, corresponding to the electrode screening frequency to avoid

*To whom correspondence should be addressed.

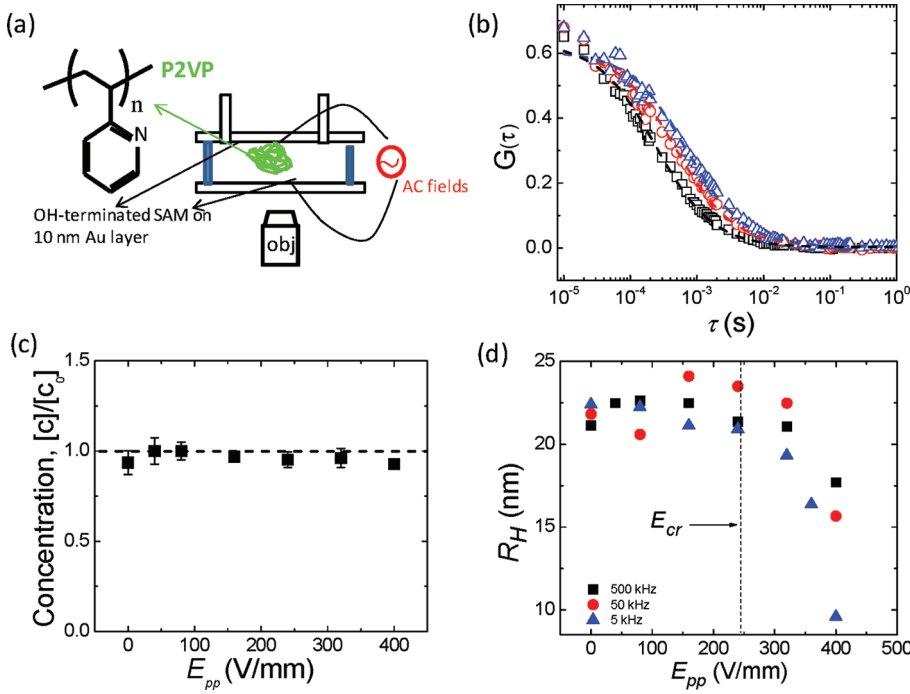


Figure 1. (a) Schematic of experimental setup using two parallel conducting surfaces to generate spatially uniform ac fields of variable ω and E_{pp} . The extended conducting surfaces are fabricated with a thin gold coating of 10 nm thick and subsequently coated with hydroxyl-terminated self-assembled monolayer to prevent P2VP from surface adsorption. (b) FCS autocorrelation function, $G(\tau)$, of fluorescence-labeled P2VP of $M_n = 135\,000$ g/mol in dilute aqueous solutions of pH = 4.16 without ac field (triangles) and under ac fields of $E_{pp} = 320$ V/mm (circles) and 400 V/mm (squares) at $\omega = 10$ kHz. Diffusion coefficient, D , and molar concentration, $[c]$, of fluorescent P2VP chains under varied ac fields are obtained by fitting $G(\tau)$ with Supporting Information eq 1. (c) Representative normalized P2VP concentration by $[c_0]$ without ac field vs E_{pp} at $\omega = 10$ kHz, indicating no P2VP concentration change or aggregation under varied uniform ac fields. (d) Measured R_H of P2VP chains pH = 4.16 vs E_{pp} at $\omega = 500$ kHz (squares), 50 kHz (circles), and 5 kHz (triangles), according to measured D . The dash line indicates the critical E_{cr} to induce the CGT of P2VP chain in dilute aqueous solutions.

P2VP electrochemical adsorption on electrodes and the inverse charge relaxation frequency, ω_C , for a P2VP coil, respectively; it should also be noted that no electrode corrosion is observed microscopically after the experiment (see detailed discussion in Supporting Information). We first investigate the conformational dynamics of single P2VP coiled chains in response to uniform ac fields of varied E_{pp} at $\omega = 10$ kHz. $G(\tau)$ obtained by FCS at $E_{pp} \leq 240$ V/mm (data not shown) overlaps with the one in the absence of ac fields as shown in Figure 1b, giving $D = 9.7 \mu\text{m}^2/\text{s}$ for P2VP chains by fitting the measured $G(\tau)$ with the following equation

$$G(\tau) = ([c]\pi^{1.5}\bar{\omega}^2 z)^{-1} \left(1 + \frac{4D\tau}{\bar{\omega}^2}\right)^{-1} \left(1 + \frac{4D\tau}{z^2}\right)^{-0.5} \quad (2)$$

which corresponds to P2VP coils of $R_H = 22.5$ nm. As shown in Figure 1b, increasing E_{pp} leads to the shift of $G(\tau)$ to shorter lag time, suggesting faster diffusion of P2VP chains. For instance, D increases to 13.3 and $22.7 \mu\text{m}^2/\text{s}$ at $E_{pp} = 320$ and 400 V/mm, corresponding to partially collapsed P2VP globules of $R_H = 16.4$ and 9.6 nm, respectively. It should be noted that all $G(\tau)$ are fitted well with eq 2, featuring the unperturbed diffusion without detectable ac-electrokinetic-induced polymer flow^{25,26} or ac-field-induced detachment of Alexa Fluor 488 from P2VP chains. Additionally, control experiments with free Alexa Fluor 488 in a dilute aqueous solution under ac fields show no change in the measured D ($\approx 220 \mu\text{m}^2/\text{s}$) of free dyes with varied ω and E_{pp} . Furthermore, as shown in Figure 1c, the uniform ac field is further verified by constant P2VP concentration, $[c]$, obtained by fitting $G(\tau)$ with eq 2. As summarized in Figure 1d, the measured R_H against E_{pp} at $\omega = 5$, 50, and 500 kHz clearly exhibit the transition from P2VP coils of $R_H = 22.5$ nm to fully collapsed globules of $R_H = 8$ nm; the critical ac field strength, E_{cr} , is thus determined as the lowest E_{pp} value where the onset of the P2VP CGT is

observed as gradually increasing E_{pp} and found around 240 ± 40 V/mm for all varied ω . It is hence expected that at an applied ac field of $E_{pp} > E_{cr} \approx 240 \pm 40$ V/mm, localized counterions can migrate away from the P2VP chain by a distance of several Bjerrum length, l_B , in a half-cycle, which involves in a possible mechanism for the observed CGT as further discussed below.

At constant $E_{pp} = 400$ V/mm $> E_{cr}$, we examine the CGT of P2VPs in response to decreased ω from 10 MHz to 5 kHz. As shown in Figure 2a, $G(\tau)$ shifts to shorter lag time scales as ω decreases to 50 and 5 kHz, indicating increased D to 21.6 and $30.4 \mu\text{m}^2/\text{s}$, respectively. At $\omega = 5$ kHz, measured D is kept constant at $30.4 \mu\text{m}^2/\text{s}$, corresponding to $R_H = 8$ nm, indicating a fully collapsed globule conformation of P2VP chains. As summarized in Figure 2b, the increase in D with decreasing ω clearly indicates an induced CGT of P2VP chains under uniform ac fields as bulk pH approximates $\text{pH}_{CGT} = 4.2$. However, it is intriguing to see a gradual and continuous CGT as ω decreases, in stark contrast to the first-order CGT by varying the pH of P2VP solutions.¹⁹

This reversible ac-field-induced CGT of P2VP is also verified at $M_n = 750\,000$ g/mol with a higher $E_{cr} \approx 400 \pm 40$ V/mm as shown in Figure 3a. As M_n is changed from 135 000 to 750 000 g/mol (equivalent to P2VP polymerization degree, N , from 1280 to 7140), E_{cr} appears to fall into a possible power law of $E_{cr} \sim N^{1/4}$ as shown in Figure 3b, different from the scaling of $E_{cr} \sim N^{-1}$ for dc-field-induced stretching^{5,27} of a collapsed polyelectrolyte chain. It should be noted that we have also examined the P2VP of $M_n = 52\,000$ g/mol, whose CGT is continuous as varying pH and sharply distinct from the behavior observed with P2VP of higher M_n , and no ac-field-induced CGT is observed at this low M_n under the same experimental conditions, which we contribute to the difference in counterion condensation and local pH gradient at varied M_n . We expect that higher degree of counterion condensation with increased M_n is contributed to the monotonic

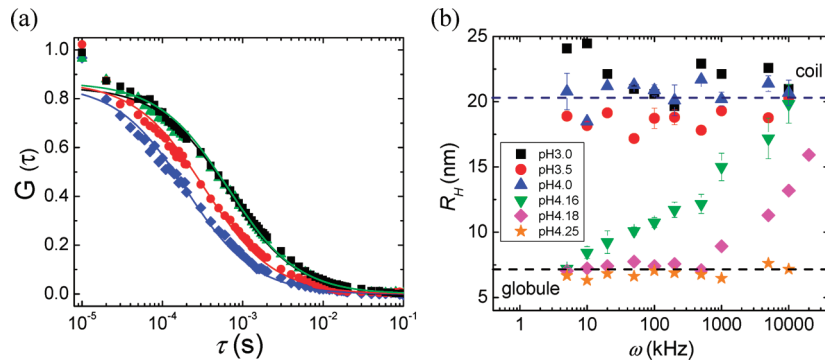


Figure 2. (a) $G(\tau)$ of P2VP chains in dilute solutions of pH = 4.16 without ac field (triangles) and under ac fields of $\omega = 10$ MHz (squares), 50 kHz (circles), and 5 kHz (diamonds) at $E_{pp} = 400$ V/mm. (b) Measured R_H of P2VP chains of $M_n = 135\,000$ g/mol against ω at constant $E_{pp} = 400$ V/mm in aqueous solutions of varied pH = 3.0 (squares), 3.5 (circles), 4.0 (up triangles), 4.16 (down triangles), 4.18 (diamonds), and 4.25 (stars). At pH = 4.16 and 4.18 and at $E_{pp} = 400$ V/mm, a gradual CGT is observed as decreasing ω .

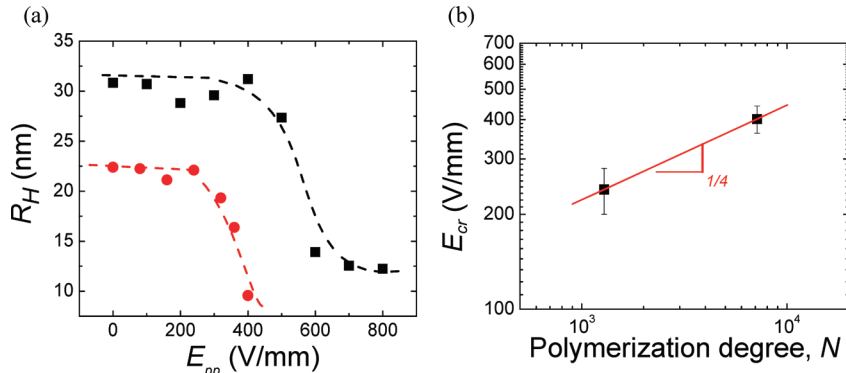


Figure 3. (a) R_H of P2VP chains of $M_n = 135\,000$ g/mol (circles) and $750\,000$ g/mol (squares) vs E_{pp} at $\omega = 50$ kHz. (b) Experimentally determined E_{cr} to induce the CGT of P2VP chain vs P2VP polymerization degree, N , in logarithmic scales. The error bar indicates the uncertainty of determined E_{cr} from repeated experiments. The slope from a linear fitting suggests a possible power law of $E_{cr} \sim N^{1/4}$.

M_n dependence of E_{cr} , where a stronger E_{pp} is demanded to strip a larger number of localized counterions away from a longer P2VP chain. A future study of the molecular weight dependence of E_{cr} to obtain a scaling behavior could be warranted, when a broad M_n range of P2VP polymer becomes commercially available.

It is recently reported²⁸ that fewer condensed counterions near a weak polyelectrolyte lead to a lower charge fraction along the polyelectrolyte backbone. To further examine this effect in ac-induced CGT of P2VP in aqueous solutions, we repeat the experiments at varied pH = 3.0–4.25 across its pH_{CGT} = 4.20 for P2VP of $M_n = 135\,000$ g/mol. Figure 2b summarizes the measured R_H of P2VP chains against ω at constant $E_{pp} = 400$ V/mm at varied pH: At pH = 3.0–4.10, P2VP coils show little change in their conformations over $\omega = 5$ kHz–10 MHz. Similarly, at pH = 4.20–4.25, no conformational transition is observed for P2VP collapsed globules. Interestingly, when the solution pH approaches its pH_{CGT} over a narrow range of 4.15–4.18, a gradual P2VP CGT is observed at pH = 4.16 and 4.18. At both pH, the gradual CGT is also reversible with increasing ω , yet a curious hysteresis upon ω -sweep is observed (see Figure 4a). It is also intriguing to observe that at pH = 4.18 the CGT is complete at $\omega \approx 1$ MHz, below which P2VP chains maintain a fully collapsed globule conformation of $R_H = 8$ nm, while at pH = 4.16, the induced CGT is progressed at a much slower pace without completing the CGT until $\omega = 5$ kHz. This observation suggests that the ac-induced local pH variation, i.e., local proton concentration variation, clearly causes counterion dissociation and migration to modify the P2VP charge density.

To verify the observed hysteresis, we repeatedly sweep ω in different directions over the range of 5 kHz–10 MHz at $E_{pp} = 400$ V/mm. A time interval of at least 5 min is waited between two

successive sweeps to allow PV2P chain relaxation. As shown in Figure 4a, the hysteresis in the ac-induced CGT is clearly observed at the constant pH = 4.16 and 4.18, showing a strong dependence with initial P2VP conformations.

Hence, for the first time, the thermal noise-driven CGT of a weak polyelectrolyte chain is reversibly and continuously controlled under spatially uniform ac fields. We further seek a quantitative understanding from MD simulation²⁹ and simple mean-field theories. On the basis of our observations, we surmise that the charge fraction of a weak hydrophobic polyelectrolyte such as P2VP is ω -dependent, such that its free energy, $W(R)$, at a given radius, R , under ac field can be described as

$$W(R) = \frac{3}{2} k_B T \left(\frac{R^2}{a^2 N} + \frac{a^2 N}{R^2} \right) + 4\pi\epsilon R^3 K(\omega) E^2 + k_B T \left(\nu_2 \frac{N^2}{R^3} + \nu_3 \frac{N^3}{R^6} \right) \quad (3)$$

where the first two terms denote the usual random walk entropic free energy and the last two terms denotes the two-body and three-body interaction between monomers, respectively. These last two terms are unimportant for the coil but are important for the globule. The induced dipole of a coil is $p = 4\pi\epsilon R^3 K(\omega) E$, where the complex Clausius–Mossotti factor; $K(\omega)$ is ω - and R -dependent due to dynamic double-layer charging and charge condensation/dissociation times.^{9,30} Hence, the time-averaged induced-dipole energy, $\langle pE \rangle = 4\pi\epsilon_M R^3 \text{Re}[K(\omega)] |E|^2$, is expected to be positive at low ω and negative at high ω —corresponding to positive and negative dielectrophoresis, respectively.⁹

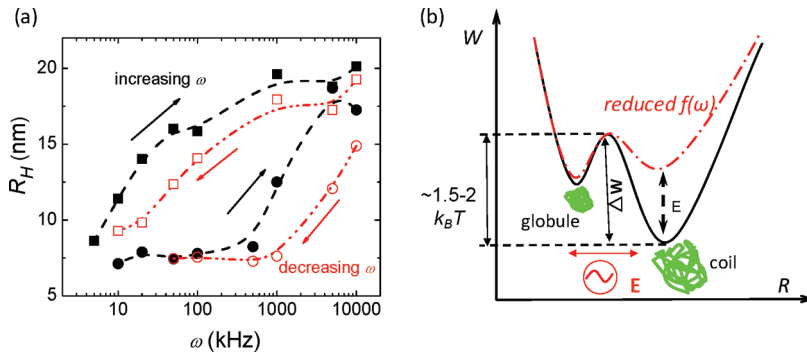


Figure 4. (a) Hysteresis of measured R_H upon ω -sweep by decreasing (open symbols) and increasing (solid symbols) ω at $E_{pp} = 400$ V/mm for $M_n = 135\,000$ g/mol at pH = 4.16 (squares) and 4.18 (circles). (b) Schematic illustration of ac-field-modified energy profile, $W(R)$, of a P2VP free chain in dilute solution at a given ω against chain radius, R , showing two energy minima corresponding to the coil and globule conformations.

The hysteretic transitions are hence expected to be near ω_C at $\text{Re}[K(\omega)] = 0$ between the inverse charge relaxation time and inverse migration times. For a hydrophobic polyelectrolyte, even without the dipole term, the signs of virial coefficients, v_2 and v_3 , allow for two energy minima—one for the coil and one for the globule, as schematically depicted in Figure 4b. The presence of an energy barrier to induce the CGT is confirmed around $1.5\text{--}2 k_B T$ by conducting a generalized ensemble Monte Carlo simulation^{17,29} (see detailed discussion in Supporting Information Figure 3). Using these field-free parameters, the ω -dependent induced dipole term (with increasing $\text{Re}[K(\omega)]$ as decreasing ω) is shown to elevate the energy of the coil minimum relative to the barrier, leading to a shift from a coil radius toward a globule radius. In the opposite direction starting with a globule conformation, decreasing $\text{Re}[K(\omega)]$ by increasing ω lowers the barrier relative to the globule minimum by the increased compression dipole force or decreased stretching force and hence again lowers the barrier height.

In summary, we observe a gradual and hysteretic CGT of a single weak polyelectrolyte chain in salt-free dilute aqueous solutions under a spatially uniform ac field. Such hysteretic transitions occur only beyond a critical field intensity that is molecular-weight-dependent and within a frequency window. The hysteresis is attributed to an asymmetric bistable energy landscape of a single hydrophobic polyelectrolyte chain, whose barrier between the coil and globule conformations can be reduced below $k_B T$ by ac-induced dipoles due to counterion dissociation, migration, and condensation. An optimum ac frequency window exists, which is determined by the inverse charge relaxation time and inverse counterion dissociation/association time scales on the polyelectrolyte backbone. Ac-induced CGT of weak polyelectrolytes can be also extended to biological polyelectrolytes and open a new route to effectively modify the chain conformations for optimal biomolecular activities, such as rapid DNA hybridization and biopolymer separation.

Acknowledgment. We gratefully acknowledge the computer simulation work and discussion by Hongjun Liu and Edward Maginn. This work is supported by the DoE-BES, Office of Basic Sciences, Division of Materials Science and Engineering (Award No. DE-FG02-07ER46390).

Supporting Information Available: Experimental details. This material is available free of charge via the Internet at <http://pubs.acs.org>.

References and Notes

- (1) Hara, M. *Polyelectrolytes*; Marcel Dekker: New York, 1993.
- (2) Barrat, J. L.; Joanny, J. F. Theory of polyelectrolyte solutions. In *Advances in Chemical Physics*; John Wiley & Sons Inc.: New York, 1996; Vol. 94, pp 1–66.
- (3) Forster, S.; Schmidt, M. Polyelectrolytes in Solution. In *Physical Properties of Polymers*; Springer-Verlag: Berlin, 1995; Vol. 120, pp 51–133.
- (4) Dobrynin, A. V.; Rubinstein, M. *Prog. Polym. Sci.* **2005**, *30*, 1049–1118.
- (5) Netz, R. R. *Phys. Rev. Lett.* **2003**, *90*, 128104.
- (6) Schroeder, C. M.; Babcock, H. P.; Shaqfeh, E. S. G.; Chu, S. *Science* **2003**, *301*, 1515–1519.
- (7) Clausen-Schaumann, H.; Rief, M.; Tolksdorf, C.; Gaub, H. E. *Biophys. J.* **2000**, *78*, 1997–2007.
- (8) Ramos, A.; Morgan, H.; Green, N. G.; Castellanos, A. *J. Phys. D: Appl. Phys.* **1998**, 2338–2353.
- (9) Basuray, S.; Chang, H. C. *Phys. Rev. E* **2007**, *75*, 060501.
- (10) Chetwani, N.; Maheshwari, S.; Chang, H. C. *Phys. Rev. Lett.* **2008**, *101*, 204501.
- (11) Mohanty, U.; Zhao, Y. Q. *Biopolymers* **1996**, *38*, 377–388.
- (12) Cohen, A. E. *Phys. Rev. Lett.* **2003**, *91*, 235506.
- (13) Washizu, H.; Kikuchi, K. *J. Phys. Chem. B* **2002**, *106*, 11329–11342.
- (14) Lifshitz, I. M.; Grosberg, A. Y.; Khokhlov, A. R. *Rev. Mod. Phys.* **1978**, *50*, 683–713.
- (15) Raphael, E.; Joanny, J. F. *Europhys. Lett.* **1990**, *13*, 623–628.
- (16) Uyaver, S.; Seidel, C. *Europhys. Lett.* **2003**, *64*, 536–542.
- (17) Yamaguchi, T.; Kiuchi, T.; Matsuoka, T.; Koda, S. *Bull. Chem. Soc. Jpn.* **2005**, *78*, 2098–2104.
- (18) Roiter, Y.; Minko, S. *J. Am. Chem. Soc.* **2005**, *127*, 15688–15689.
- (19) Wang, S.; Zhao, J. *J. Chem. Phys.* **2007**, *126*, 091104.
- (20) Melnikov, S. M.; Sergeyev, V. G.; Yoshikawa, K. *J. Am. Chem. Soc.* **1995**, *117*, 9951–9956.
- (21) Kiriy, A.; Gorodyska, G.; Minko, S.; Jaeger, W.; Stepanek, P.; Stamm, M. *J. Am. Chem. Soc.* **2002**, *124*, 13454–13462.
- (22) Sukhishvili, S. A.; Chen, Y.; Muller, J. D.; Gratton, E.; Schweizer, K. S.; Granick, S. *Macromolecules* **2002**, *35*, 1776–1784.
- (23) Magde, D.; Elson, E.; Webb, W. W. *Phys. Rev. Lett.* **1972**, *29*, 705–708.
- (24) Rigler, R.; Mets, U.; Widengren, J.; Kask, P. *Eur. Biophys. J. Biophys. Lett.* **1993**, *22*, 169–175.
- (25) Morgan, H.; Green, N. G. *AC Electrokinetic: Colloids and Nanoparticles (Microtechnologies and Microsystems)*; Research Studies Press Ltd.: England, 2003.
- (26) Kohler, R.; Schwille, P.; Webb, W.; Hanson, M. *J. Cell Sci.* **2000**, *113*, 3921–3930.
- (27) Hsiao, P. Y.; Wu, K. M. *J. Phys. Chem. B* **2008**, *112*, 13177–13180.
- (28) Wang, S.; Granick, S.; Zhao, J. *J. Chem. Phys.* **2008**, *129*, 241102.
- (29) Liu, H.; Zhu, Y.; Maginn, E. J. *Macromolecules* **2010**, *43*, 4805–4813.
- (30) Pohl, H. A. *Dielectrophoresis*; Cambridge University Press: Cambridge, 1978.